



## SENSITIVITY ANALYSIS OF OPTIMIZATION MODELS FOR TWO ADJACENT INTERSECTIONS WITH CORRELATED SHORT LEFT-TURN LANES

Ronghan Yao

*School of Transportation and Logistics, Dalian University of Technology, Dalian, 116024, China*

Submitted 22 July 2011; accepted 28 November 2011

**Abstract.** The correlated short left-turn lanes sometimes exist on the common section between two adjacent intersections. These short lanes can reduce the approach capacity and impact on each other. According to operational research, three kinds of multi-objective optimization models are put forward in order to reasonably allocate the time-space resources of two intersections. Since the solutions to these models depend on the concrete forms of their objective functions, six feasible objective functions and the corresponding solution method are proposed. Next, the sensitivity of the optimization results to the parameters (minimum and maximum cycle lengths) is emphatically analyzed and compared. Moreover, to testify the effects of these models on traffic flow operations, three typical optimization scenarios are simulated together with the existing one. The models and methods are illustrated via the 2010 field data from the city of Dalian, China. Also, the better models and their suitable parameter values or ranges are recommended. Finally, the application procedure of the recommended models is given in actual engineering practice.

**Keywords:** adjacent intersections; correlated short left-turn lanes; optimization models; sensitivity analysis.

**Reference to this paper should be made as follows:** Yao, R. 2013. Sensitivity analysis of optimization models for two adjacent intersections with correlated short left-turn lanes, *Transport* 28(3): 256–269.  
<http://dx.doi.org/10.3846/16484142.2013.829781>

### Introduction

At signalized intersections, left-turn lanes often exist in the form of short lanes. While a significant amount of research has been devoted to studying signalized intersections, only a limited number of studies exist to discuss the effect of short lanes on signalized intersection operations. In the *Highway Capacity Manual* (2000), the short left-turn lanes (SLs) are basically treated as exclusive lanes. Such a treatment neglects the potential effect of the short lanes on the approach capacity. Much existing literature for short-lane research mainly focuses on two aspects, the impact of short lanes on capacity or utilization and the determination of the lengths of short lanes.

Regarding the impact of short lanes on capacity, a German scholar Wu made a series of findings that added to the existing work in the field. He early emphasized the overestimation of the conventional methods and the underestimation of the shared lanes' formula, and proposed an analytical procedure based

on probability theory to estimate accurately the capacity of shared and short lanes (Wu 1999). Then, he and his co-operator presented a capacity estimation model to overcome one of the major shortcomings of the current capacity estimation methodologies by considering the probabilistic nature of traffic flow and the effect of queue blockage on the short-lane section. They also noted the capacity of a signalized intersection with a short right-turn lane is strongly related to the length of the short lane, the proportion of through and right-turn vehicles, and cycle length (Tian, Wu 2006). Most recently, he developed a theoretical-empirical model to estimate the total approach capacity at signalized intersections with shared short lanes by considering the stochastic nature of a traffic flow and the effect of queue blockage on the short turn lanes (Wu 2007). In addition, Jiang and Yang (2008) proposed a criterion to estimate the relationship between capacity and cycle length for a signalized intersection approach

Corresponding author: Ronghan Yao  
E-mail: [cyanyrh@dlut.edu.cn](mailto:cyanyrh@dlut.edu.cn)

with a short right-turn lane; and Klibavicius *et al.* (2008) presented a methodology for calculating the capacity of right and left short lanes depending on the length of the traffic lane. On the other hand, for the impact of short lanes on utilization, Lee *et al.* (2005) found that the short lane is typically underutilized since drivers tend to avoid using the short lane due to the potential for stressful merges downstream of the signal, and presented the models to predict lane utilization factors for six intersection types and to assess how low lane utilization affects the observed intersection capacity and level of service.

Concerning the determination of the lengths of short lanes, Kikuchi and his co-authors made very good progress. At first, they analyzed the required length of the left-turn lane at signalized intersections and gave the recommended lengths for different conditions (Kikuchi *et al.* 1993). Since then, to avoid lane overflow and blockage of lane entrance, they developed a procedure to determine the length of the double short left-turn lanes (DLTLs) (Kikuchi *et al.* 2004). They further examined the appropriate lengths of turn lanes when a single lane approaches a signalized intersection and is divided into three lanes: left-turn, through, and right-turn. The length was calculated so that the probability that lane does not overflow and a lane entrance is not blocked is greater than a threshold value (Kikuchi *et al.* 2007). Recently, they proposed an analytical procedure for determining the lengths of left-turn lanes at signalized intersections to prevent lane overflow and blockage of the entrance of the left-turn lane by the queued through vehicles (Kikuchi, Kronprasert 2010). Additionally, Qi *et al.* (2007) asserted the left-turn lane should be designed to have a length sufficient to store the longest expected queue to prevent lane overflow, and developed a new method to estimate the storage lengths of left-turn lanes at signalized intersections.

The aforementioned achievements indicate that short lanes have an important effect on intersection operations and should be well designed so as to enhance intersection capacity and level of service. The authors have put forward the models of jointly optimizing the SL lengths and the phase effective green times for isolated intersections (Yao *et al.* 2011). This paper aims to build the optimization models for two adjacent intersections with the correlated SLs on their common section, and then to analyze the sensitivity of the optimization results to the parameters so as to find the stable model and the suitable parameter value.

The following contents are organized as follows. The section entitled “Basic principle and assumptions” gives the symbols and definitions used in the paper, introduces the impact of a short lane on approach capacity, and describes the study objects in the paper. Then, the “Modeling and solving” section analyses the objectives and constraints, constructs three kinds of multi-objective optimization models,

and presents the solution method. By using the field data from the city of Dalian, China, the sensitivity of the optimization results to the model parameters (critical cycle lengths) is analyzed in the “Sensitivity analysis of optimization results to model parameters” section. To further study the effects of different scenarios on traffic flow operations, the current scenario and three characterized optimization scenarios are simulated by utilizing VISSIM software, and the corresponding traffic flow operations are evaluated and compared by adopting the node and link evaluations in VISSIM in the section titled “Model verification and validation”. Next, the section entitled “Model application” discusses the optimization and simulation outcomes ahead, proposes the recommended objective functions and the corresponding critical cycle lengths, and puts forward the procedure of using the recommended models, so as to solve the common multi-period signal timing problem. Finally, the main contribution of this work in theoretical and practical advancement is summarized in the “Conclusions” section.

## 1. Basic principle and assumptions

### 1.1. Symbols and definitions

The following symbols and definitions are used in this paper:

- $q_{ij}^n$  – arrival flow rate for lane group  $j$  in phase  $i$  at intersection  $\eta$  (veh/h);
- $S_{fij}^n$  – saturation flow rate for the full lanes in lane group  $j$  in phase  $i$  at intersection  $\eta$  (veh/h);
- $S_{sij}^n$  – saturation flow rate for the short lane in lane group  $j$  in phase  $i$  at intersection  $\eta$  (veh/h);
- $y_{ij}^n$  – flow ratio for lane group  $j$  in phase  $i$  at intersection  $\eta$ ;
- $y_i^n$  – flow ratio for phase  $i$  at intersection  $\eta$ ;
- $Y^n$  – total flow ratio for intersection  $\eta$ ;
- $L^n$  – total lost time for intersection  $\eta$  (s);
- $D_{ij}^n$  – length of the short lane in lane group  $j$  in phase  $i$  at intersection  $\eta$  (m);
- $\delta_{ij}^n$  – identifier for the short lane in lane group  $j$  in phase  $i$  at intersection  $\eta$ , if yes,  $\delta_{ij}=1$ , or else,  $\delta_{ij}=0$ ;
- $h$  – average queue spacing between a pair of vehicles (m);
- $t$  – average saturation headway between a pair of vehicles (s);
- $g_{ij}^n$  – queue full discharge time for the short lane in lane group  $j$  in phase  $i$  at intersection  $\eta$  (s);
- $g_i^n$  – effective green time for phase  $i$  at intersection  $\eta$  (s);
- $m_i^n$  – number of lane groups in phase  $i$  at intersection  $\eta$ ;
- $n^n$  – number of phases for intersection  $\eta$ ;
- $C^n$  – cycle length for intersection  $\eta$  (s);
- $u_i^n$  – green ratio for phase  $i$  at intersection  $\eta$ ;
- $x_{ij}^n$  – degree of saturation for a lane group  $j$  in phase  $i$  at intersection  $\eta$ ;
- $x^n$  – degree of saturation for intersection  $\eta$ ;

- $Q_{ij}^n$  – capacity of lane group  $j$  in phase  $i$  at intersection  $\eta$  (veh/h);
- $Q^n$  – capacity of intersection  $\eta$  (veh/h);
- $d_{ij}^n$  – unit control delay for lane group  $j$  in phase  $i$  at intersection  $\eta$  (s/veh);
- $d_{1ij}^n$  – uniform control delay for lane group  $j$  in phase  $i$  at intersection  $\eta$  (s/veh);
- $d_{2ij}^n$  – incremental delay for lane group  $j$  in phase  $i$  at intersection  $\eta$  (s/veh);
- $d_{3ij}^n$  – initial queue delay for lane group  $j$  in phase  $i$  at intersection  $\eta$  (s/veh);
- $PF$  – uniform delay progression adjustment factor;
- $T$  – duration of analysis period (h);
- $k$  – incremental delay factor that is dependent on controller settings;
- $I$  – upstream filtering or metering adjustment factor;
- $d^n$  – unit delay for total vehicles pass through intersection  $\eta$  (s/veh);
- $g_{\min i}^n$  – minimum effective green time for phase  $i$  at intersection  $\eta$  (s);
- $g_{\max i}^n$  – maximum effective green time for phase  $i$  at intersection  $\eta$  (s);
- $C_{\min}^n$  – minimum cycle length for intersection  $\eta$  (s);
- $C_{\max}^n$  – maximum cycle length for intersection  $\eta$  (s);
- $D_{\max ij}^n$  – maximum channelization length of the short lane in a lane group  $j$  in phase  $i$  at intersection  $\eta$  (m), and can adopt the length of segment between two neighboring intersections;
- $D_0$  – length of the common section between two adjacent intersections (m).

**1.2. Impact of a short lane on approach capacity**

As shown in Fig. 1, there are two full lanes (FLs) and one SL in the same lane group on an approach. The saturation flow rates for the FLs and SL in the lane group are  $S_f$  and  $S_s$ , respectively. Assume that the queue full discharge time for the SL is  $g_s$  and the effective green time is  $g$  in the study phase. When the signal light of this phase turns green, the vehicles on the three lanes are released with the duration of  $g_s$ . After that, the vehicles on the two FLs are only discharged with the duration of  $g - g_s$ . That is to say, the approach saturation flow rate is not a constant and decreases from  $S_f + S_s$  to  $S_f$ . During the

effective green time  $g$ , the equivalent constant saturation flow rate can be denoted as  $S$  for the approach and  $S = S_f + S_s \cdot g_s/g$ . Note that  $g_s = D \cdot t/h \leq g$  here.

On the one hand, if the cycle length for a given intersection is longer, the related effective green time may be longer than the queue full discharge time for the short lane, then the saturation flow rate of the corresponding approach can decrease. As a result, the intersection capacity correspondingly descends. On the other hand, because lost time is experienced with each start and stop of a movement, the total amount of time lost over an hour is related to the signal timing. If the cycle length for a given intersection is shorter, the times of start and stop for each movement are larger so that the total lost time during an hour is greater for all traffic movements. Accordingly, the intersection capacity decreases along with cycle length shortening. Comparing these two aspects, there should be an optimal channelization and signal timing design to maximize the intersection capacity. When two adjacent intersections are studied, there should also be an optimum combination of channelization and signal timing to maximize the total capacity for these two intersections as a whole.

**1.3. Case description**

In this paper, we discuss the case of channelizing the SLs on the approaches of the common section between two adjacent intersections, as shown in Fig. 2. Moreover, the SLs may be also channelized on any other approaches. Here  $D^a$  and  $D^b$  represent the lengths of the correlated SLs for intersections  $a$  and  $b$ , respectively, and  $D_0$  refers to the length of the common section between intersections  $a$  and  $b$ . In the figure, each intersection is a four-leg intersection and each branch includes an approach and an exit. This figure can be simplified in the following way. For intersection  $a$  or  $b$  (or both), there may be one or two approaches (on different streets) or one branch missing, except from on the common section. When one branch is missing, the intersection will be a three-leg intersection. In addition, each intersection splits two, three or four phases.

Another condition for this study is that these two intersections are not coordinated by traffic

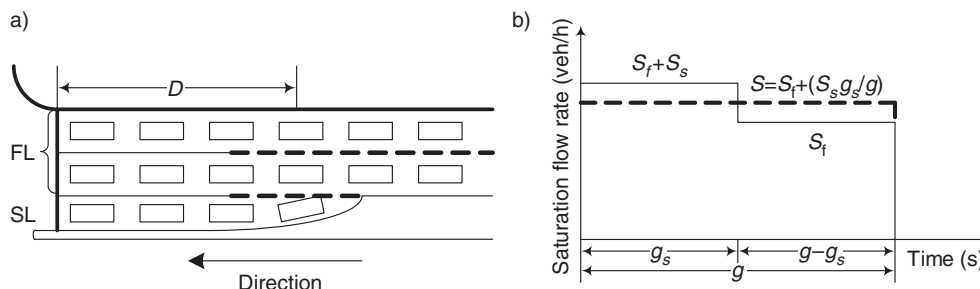


Fig. 1. Impact of a short lane on saturation flow rate of the approach: a – a short left-turn lane on approach; b – time-dependent curve of saturation flow rate

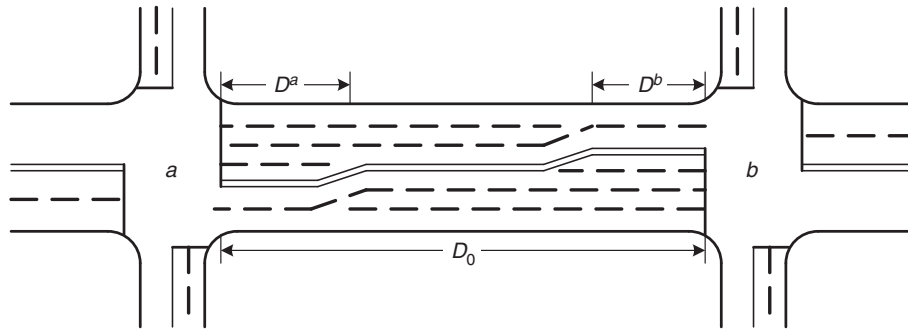


Fig. 2. Channelization scheme for two adjacent intersections

signals, that is to say, they can be treated as isolated intersections. There are two situations which correspond with this condition. One is that any of traffic movements at one intersection has no impact on any of the ones at another intersection. “Guidelines for Traffic Signals” (Road and Transportation Research Association 2003) denoted that “Green Waves for motorized traffic are recommended for a traffic signal spacing of up to 750 metres, under particularly favorable conditions up to 1000 metres”. Thus, the other is that the distance between a pair of adjacent intersections is longer than 750–1000 metres. The essence of these two cases is that there is no relativity between any of the traffic movements at one intersection and any of ones at another intersection.

**2. Modeling and solving**

**2.1. Objectives**

For urban intersections, planners, designers, or managers from the departments related to transportation and traffic pursue maximizing the system performance, measured, for example, by the capacity that is the most widely used, whereas, users or travelers including drivers, bicyclists, and pedestrians aim to minimize their travel delay. In the following subsection, three kinds of multi-objective optimization models will be developed.

Capacity at intersections is defined for each lane group. The lane group capacity is the maximum hourly rate at which vehicles can reasonably be expected to pass through the intersection under prevailing traffic, roadway, and signalization conditions in the *Highway Capacity Manual (2000)*. The intersection capacity is the sum of all lane group capacity.

Based on the analysis in the above section, the capacity of a given lane group for a study intersection is expressed as:

$$Q_{ij}^n = \begin{cases} (S_{ij}^n \cdot g_i^n + \delta_{ij}^n \cdot S_{sij}^n \cdot g_{ij}^n) / C, & g_i^n \geq g_{ij}^n; \\ (S_{ij}^n \cdot g_i^n + \delta_{ij}^n \cdot S_{sij}^n \cdot g_{ij}^n) / C, & g_i^n < g_{ij}^n, \end{cases} \quad \eta \in \{a, b\}. \quad (1)$$

The capacity of all the lane groups can be aggregated to provide the capacity of a specified intersection, as computed using:

$$Q^\eta = \sum_{i=1}^{n^\eta} \sum_{j=1}^{m_i^\eta} Q_{ij}^\eta, \quad \eta \in \{a, b\}, \quad (2)$$

where:

$$C^\eta = \sum_{i=1}^{n^\eta} g_i^\eta + L^\eta; \quad g_{ij}^\eta = \frac{D_{ij}^\eta \cdot t}{h}.$$

The average control delay per vehicle for a given lane group is given by the *Highway Capacity Manual (2000)*, as indicated in the following equation:

$$d_{ij}^\eta = d_{1ij}^\eta \cdot (PF) + d_{2ij}^\eta + d_{3ij}^\eta, \quad \eta \in \{a, b\}. \quad (3)$$

The control delays for all the lane groups can be aggregated to provide the average control delay for the intersection as a whole, as calculated using:

$$d^\eta = \frac{\sum_{i=1}^{n^\eta} \sum_{j=1}^{m_i^\eta} q_{ij}^\eta d_{ij}^\eta}{\sum_{i=1}^{n^\eta} \sum_{j=1}^{m_i^\eta} q_{ij}^\eta}, \quad \eta \in \{a, b\}, \quad (4)$$

where:

$$d_{1ij}^\eta = \frac{0.5 \cdot C^\eta \cdot (1 - u_i^\eta)^2}{1 - \min(1, x_{ij}^\eta) \cdot u_i^\eta};$$

$$d_{2ij}^\eta = 900 \cdot T \times \left( (x_{ij}^\eta - 1) + \sqrt{(x_{ij}^\eta - 1)^2 + \frac{8 \cdot k \cdot I \cdot x_{ij}^\eta}{Q_{ij}^\eta \cdot T}} \right);$$

$$u_i^\eta = \frac{g_i^\eta}{C^\eta}; \quad x_{ij}^\eta = \frac{q_{ij}^\eta}{Q_{ij}^\eta}.$$

**2.2. Constraints**

Firstly, to exert the short lane and to avoid lane overflow and blockage of lane entrance, the phase effective green time should be equal to or greater than the queue full discharge time for the short lane, namely:

$$g_i^\eta \geq g_{ij}^\eta, \quad \forall \delta_{ij}^\eta = 1, \quad \eta \in \{a, b\}. \quad (5)$$

Secondly, those two correlated short lanes on the common section should satisfy:

$$D_{kl}^a + D_{mn}^b \leq D_0, \quad \forall \delta_{kl}^a = 1, \quad \delta_{mn}^b = 1. \quad (6)$$

Thirdly, the phase effective green time should be between the critical upper and lower bounds, that is:

$$g_{\min i}^\eta \leq g_i^\eta \leq g_{\max i}^\eta, \quad \eta \in \{a, b\}. \quad (7)$$

According to the equal degree of saturation principle, the minimum and maximum phase effective green times can be computed by the following equations:

$$g_{\min i}^\eta = \frac{y_i^\eta}{Y^\eta} \cdot (C_{\min}^\eta - L^\eta), \quad \eta \in \{a, b\}, \quad (8)$$

$$g_{\max i}^\eta = \frac{y_i^\eta}{Y^\eta} \cdot (C_{\max}^\eta - L^\eta), \quad \eta \in \{a, b\}. \quad (9)$$

Finally, the short lane length should be between the reasonable upper and lower bounds, as shown in the following equation:

$$0 \leq D_{ij}^\eta \leq D_{\max ij}^\eta, \quad \forall \delta_{ij}^\eta = 1, \quad \eta \in \{a, b\}. \quad (10)$$

### 2.3. Optimization models

When maximizing intersection capacity from the managers' perspective, the optimization problem is to maximize the objective function of equation (2) under the constraints of equations (5)–(7) and (10), so we have:

$$\begin{aligned} & \text{maximize } Q^\eta = \sum_{i=1}^{n^\eta} \sum_{j=1}^{m_i^\eta} Q_{ij}^\eta, \quad \eta \in \{a, b\} \\ & \text{subject to: } g_i^\eta \geq \frac{D_{ij}^\eta t}{h}, \quad \forall \delta_{ij}^\eta = 1, \\ & \quad D_{kl}^a + D_{mn}^b \leq D_0, \quad \forall \delta_{kl}^a = 1, \quad \delta_{mn}^b = 1, \\ & \quad \frac{y_i^\eta}{Y^\eta} \cdot (C_{\min}^\eta - L^\eta) \leq g_i^\eta \leq \frac{y_i^\eta}{Y^\eta} \cdot (C_{\max}^\eta - L^\eta), \\ & \quad 0 \leq D_{ij}^\eta \leq D_{\max ij}^\eta, \quad \forall \delta_{ij}^\eta = 1. \end{aligned} \quad (11)$$

On the other hand, when minimizing intersection control delay from the users' perspective, the optimization problem is to minimize the objective function of equation (4) under the constraints of equations (5)–(7) and (10), so we have:

$$\begin{aligned} & \text{minimize } d^\eta = \frac{\sum_{i=1}^{n^\eta} \sum_{j=1}^{m_i^\eta} q_{ij}^\eta d_{ij}^\eta}{\sum_{i=1}^{n^\eta} \sum_{j=1}^{m_i^\eta} q_{ij}^\eta}, \quad \eta \in \{a, b\} \\ & \text{subject to: } g_i^\eta \geq \frac{D_{ij}^\eta \cdot t}{h}, \quad \forall \delta_{ij}^\eta = 1, \\ & \quad D_{kl}^a + D_{mn}^b \leq D_0, \quad \forall \delta_{kl}^a = 1, \quad \delta_{mn}^b = 1, \\ & \quad \frac{y_i^\eta}{Y^\eta} \cdot (C_{\min}^\eta - L^\eta) \leq g_i^\eta \leq \frac{y_i^\eta}{Y^\eta} \cdot (C_{\max}^\eta - L^\eta), \\ & \quad 0 \leq D_{ij}^\eta \leq D_{\max ij}^\eta, \quad \forall \delta_{ij}^\eta = 1. \end{aligned} \quad (12)$$

If maximizing capacity and minimizing control delay for given intersections simultaneously, the optimization problem becomes to maximize equation

(2) and minimize equation (4) under the constraints of equations (5)–(7) and (10), then the optimization model becomes:

$$\begin{aligned} & \text{maximize } Q^\eta = \sum_{i=1}^{n^\eta} \sum_{j=1}^{m_i^\eta} Q_{ij}^\eta, \quad \eta \in \{a, b\} \\ & \text{minimize } d^\eta = \frac{\sum_{i=1}^{n^\eta} \sum_{j=1}^{m_i^\eta} q_{ij}^\eta d_{ij}^\eta}{\sum_{i=1}^{n^\eta} \sum_{j=1}^{m_i^\eta} q_{ij}^\eta}, \quad \eta \in \{a, b\} \\ & \text{subject to: } g_i^\eta \geq \frac{D_{ij}^\eta \cdot t}{h}, \quad \forall \delta_{ij}^\eta = 1, \\ & \quad D_{kl}^a + D_{mn}^b \leq D_0, \quad \forall \delta_{kl}^a = 1, \quad \delta_{mn}^b = 1, \\ & \quad \frac{y_i^\eta}{Y^\eta} \cdot (C_{\min}^\eta - L^\eta) \leq g_i^\eta \leq \frac{y_i^\eta}{Y^\eta} \cdot (C_{\max}^\eta - L^\eta), \\ & \quad 0 \leq D_{ij}^\eta \leq D_{\max ij}^\eta, \quad \forall \delta_{ij}^\eta = 1. \end{aligned} \quad (13)$$

### 2.4. Model solutions

Equation (11) is a double-objective optimization problem. According to operations research, because the units of capacity of intersections  $a$  and  $b$  are the same, we apply the weighted method to convert two targets into a single target in order to solve it.

Equation (12) is also a double-objective optimization problem. Similarly, because the units of delays for intersections  $a$  and  $b$  are identical, we also apply the weighted method to convert two targets into a single target so as to solve it.

Equation (13) is a four-objective optimization problem. Since the units of capacity and delay are different, we combine the weighted method and the multiplication or division method to convert four targets into a single target in order to resolve it.

Based on the above analysis, there are six specific objective functions in all, as listed in Table 1, together with their codes. When a multi-objective optimization problem is transformed into a single-objective one, we can apply the *fmincon* function in the *MATLAB* to find a constrained minimum of a function with several variables.

## 3. Sensitivity analysis of optimization results to model parameters

According to the section ahead, equations (11), (12) and (13) are all nonlinear optimization problems with constraints. Also, the two objective functions in equation (13) are not independent because capacity is included in the delay formula, as indicated in equation (3). On the other hand, cycle length should be within a reasonable range for an intersection on the basis of the current researches. Therefore, we will adopt the enumeration method to analyze the sensitivity of the optimization results to the model parameters for equations (11), (12) and (13) here.

### 3.1. Data source

To testify the given optimization models, researchers surveyed two consecutive hours during the weekday

Table 1. Concrete objective functions and their codes

| Objective function                   | Code of objective function | Objective function                   | Code of objective function |
|--------------------------------------|----------------------------|--------------------------------------|----------------------------|
| maximize $(Q_A + Q_B)$               | OF1                        | minimize $(d_A + d_B) / (Q_A + Q_B)$ | OF4                        |
| minimize $(d_A + d_B)$               | OF2                        | maximize $(Q_A d_A + Q_B d_B)$       | OF5                        |
| maximize $(Q_A + Q_B) / (d_A + d_B)$ | OF3                        | minimize $(d_A / Q_A + d_B / Q_B)$   | OF6                        |

morning peak period at the intersections of Zhongshan Road & Youhao Street and Changjiang Road & Youhao Street, denoted as  $a$  and  $b$ , in the city of Dalian, China in 2010.

Fig. 3a shows a photo for these two intersections. Fig. 3b illustrates the channelization scheme for the selected intersections. At intersection  $a$ , four through lanes and a right-turn lane are included on the eastbound and westbound approaches, and two left-turn lanes, a shared through-left lane and two through lanes are contained on the southbound approach, where a SL is channelized with the length of 66 metres. At intersection  $b$ , four through lanes are comprised on the westbound approach, three through lanes and a right lane are involved on the eastbound approach, two left-turn lanes and a shared left-right lane are covered on the northbound approach, where a SL is channelized with the length of 33 metres. The common section between intersections  $a$  and  $b$  is 185 metres. Fig. 3c depicts the signal phase plan for the selected intersections. Two phases are designed at each intersection. At intersection  $a$ , the first is the eastbound and westbound through movements, the second is the southbound through and left-turn movements; the cycle length is 120 seconds, the green times of the first and second phases are 79 and 31 seconds, respectively. At intersection  $b$ , the first is the eastbound and westbound through movements, the second is the northbound left-turn movement; the cycle length is 73 seconds, the green times of the first and second phases are 50 and 13 seconds, respectively. In addition, the amber time is 3 seconds for each phase.

Based on the data processing and analysis, Table 2 lists the saturation flow rates, the peak 5-min flow rates, and the hourly volumes for each lane group on each approach at the observed signalized intersections.

### 3.2. Calibration of parameters

As is stated before, some parameters need to be calibrated when the delay formula from the Highway Capacity Manual (2000) is used. Therefore, the values of these parameters are given as follows.

First, based on the actual traffic composition, a value of  $PF = 1.0$  is used for which traffic arrivals are random. Next, according to the observations, there was no residual queue from a previous period at the start of the analysis period for each intersection. Therefore,  $d_{3ij}^a$  and  $d_{3ij}^b$  are all zero. Then, the duration of analysis period is one hour in this paper, and thus  $T$  is set to 1.0. At last, these two observed intersections were all controlled by the pre-timed signals and were not coordinated with each other. Thus, they could be regarded as isolated intersections. Then, a value of 0.5 for  $k$  and a value of 1.0 for  $I$  are used.

In addition, the start-up lost time per phase and the all-red time between two adjacent phases are individually set to 1.47 seconds and 2 seconds on the basis of the survey data (Yao *et al.* 2011). Thus, the total lost time per phase is 3.47 seconds.

### 3.3. Sensitivity of optimization results to critical cycle lengths

In the Highway Capacity Manual (2000), the recommended minimum and maximum cycle lengths are 60 and 150 seconds, respectively. In the “Traffic Management and Control”, the suitable range of cycle length is given to be 40–180 seconds, and the cycle length should not be greater than 120 seconds during peak hours (Wu, Li 2009). Considering the current cycle lengths and total flow ratios for intersections  $a$  and  $b$ , the range of cycle length is set to 40–120 seconds here.

For objective function OF1, the minimum and maximum cycle lengths have a significant effect on the optimization results. If a given range of cycle length is not suitable for a specified intersection, although an optimal intersection capacity can be attained, the control delay may be huge and the degree of saturation may be greater than 1. In this case, the operation conditions for traffic stream are much worse. By testing, the suitable ranges of cycle lengths for intersections  $a$  and  $b$  are individually 60–80 and 40–80 seconds, so as to attain the maximum capacity under the conditions of which the degrees of saturation for these two intersections are both less than 1. At this time, the optimization results are listed as OP1 in Table 3.

For objective functions OF2 through OF6, Table 3 also indicates the optimization values and evaluation indices under different critical cycle lengths for intersections  $a$  and  $b$ . For intersection  $a$ , the optimization outcomes of OF2, OF3 and OF5 are all stable and very close under any critical cycle lengths; the capacity of OF2 is the least, but its capacity to delay ratio is the most; the capacity of OF5 is the most, but its capacity to delay ratio is the least; the capacity and capacity to delay ratio of OF3 is medium; the optimization outcomes of OF4 and OF6 are very close and strongly depend on the minimum cycle length under any critical cycle lengths, the lesser the minimum cycle length, the

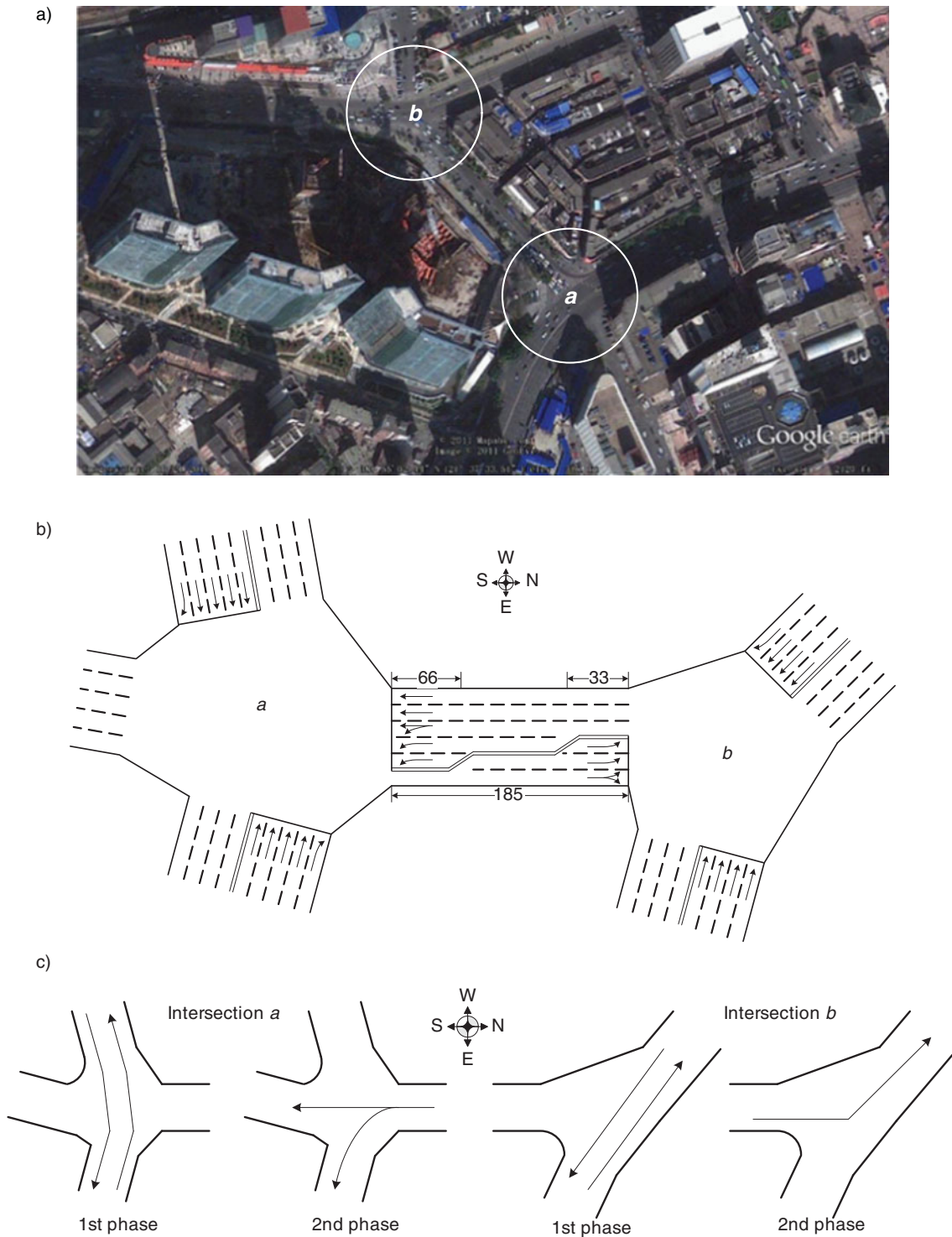


Fig. 3. Illustrations for the existing intersections: a – photograph; b – channelization scheme; c – signal phase scheme

more the capacity to delay ratio. For intersection *b*, the optimization outcomes of all objective functions strongly depend on the minimum cycle length, the optimization outcomes of OF2, OF3 and OF5 are very close, and those of OF4 and OF6 are very close under any critical cycle lengths.

On the whole, equation (11) is hard to use because of being sensitive; equations (12) and (13)

are easy to use because of being stable and the suitable range of critical cycle lengths is 40÷120 s. By comparing the total capacity to delay ratios, OP12 is the best when optimizing objective functions OF2, OF3 and OF5; OP16 is the best when optimizing objective functions OF4 and OF6. Moreover, for the close optimization scenarios, for example, OP14 and OP16, they are the same in actual application.

Table 2. Saturation flow rates, peak 5-min flow rates and volumes

| Intersection | Traffic flow parameters (veh/h)      | Westbound approach | Eastbound approach | Northbound approach | Southbound approach |
|--------------|--------------------------------------|--------------------|--------------------|---------------------|---------------------|
| <i>a</i>     | Saturation flow rates of full lanes  | 6743               | 7189               | –                   | 6556                |
|              | Saturation flow rates of short lanes | –                  | –                  | –                   | 1679                |
|              | Peak 5-min flow rates                | 3102               | 4278               | –                   | 2148                |
|              | Hourly volumes                       | 2563               | 3486               | –                   | 1751                |
| <i>b</i>     | Saturation flow rates of full lanes  | 5697               | 4713               | 3178                | –                   |
|              | Saturation flow rates of short lanes | –                  | –                  | 1567                | –                   |
|              | Peak 5-min flow rates                | 1812               | 2328               | 918                 | –                   |
|              | Hourly volumes                       | 1228               | 1660               | 613                 | –                   |

Table 3. Model optimization outcomes under different critical cycle lengths

| CS   | COF | $C_{min}$ (s) | $C_{max}$ (s) | Intersection | $D$ (m) | $g_1$ (s) | $g_2$ (s) | $C$ (s) | $Q$ (veh/h) | $d$ (s/veh) | $x$  | $Q/d$   | $\Sigma Q/d$ |
|------|-----|---------------|---------------|--------------|---------|-----------|-----------|---------|-------------|-------------|------|---------|--------------|
| OP1  | OF1 | 60            | 80            | <i>a</i>     | 48.51   | 50.80     | 16.17     | 73.91   | 11,377      | 17.31       | 0.97 | 657.22  | 1244.72      |
|      |     | 40            | 80            | <i>b</i>     | 27.91   | 52.50     | 9.30      | 68.74   | 8592        | 14.63       | 0.95 | 587.50  |              |
| OP2  | OF2 | 60            | 120           | <i>a</i>     | 59.58   | 44.70     | 19.86     | 71.50   | 10,997      | 13.74       | 0.78 | 800.13  | 1682.50      |
|      |     | 60            | 120           | <i>b</i>     | 44.80   | 38.13     | 14.93     | 60.00   | 7796        | 8.84        | 0.55 | 882.38  |              |
| OP3  | OF3 | 60            | 120           | <i>a</i>     | 61.98   | 46.68     | 20.66     | 74.28   | 11,046      | 14.07       | 0.77 | 785.26  | 1671.66      |
|      |     | 60            | 120           | <i>b</i>     | 44.80   | 39.61     | 14.93     | 61.48   | 7859        | 8.87        | 0.55 | 886.40  |              |
| OP4  | OF4 | 60            | 120           | <i>a</i>     | 18.00   | 36.89     | 16.17     | 60.00   | 10,501      | 13.78       | 0.91 | 762.18  | 1576.90      |
|      |     | 60            | 120           | <i>b</i>     | 18.00   | 38.13     | 14.93     | 60.00   | 7563        | 9.28        | 0.65 | 814.72  |              |
| OP5  | OF5 | 60            | 120           | <i>a</i>     | 62.21   | 46.87     | 20.74     | 74.54   | 11,050      | 14.10       | 0.77 | 783.81  | 1669.28      |
|      |     | 60            | 120           | <i>b</i>     | 44.80   | 39.22     | 14.93     | 61.09   | 7843        | 8.86        | 0.55 | 885.47  |              |
| OP6  | OF6 | 60            | 120           | <i>a</i>     | 18.38   | 36.89     | 18.74     | 62.58   | 10,342      | 13.96       | 0.82 | 741.08  | 1533.78      |
|      |     | 60            | 120           | <i>b</i>     | 18.23   | 38.13     | 15.72     | 60.79   | 7508        | 9.47        | 0.63 | 792.70  |              |
| OP7  | OF2 | 50            | 120           | <i>a</i>     | 59.57   | 44.70     | 19.86     | 71.50   | 10,997      | 13.74       | 0.78 | 800.14  | 1753.65      |
|      |     | 50            | 120           | <i>b</i>     | 36.36   | 30.94     | 12.12     | 50.00   | 7592        | 7.96        | 0.57 | 953.51  |              |
| OP8  | OF3 | 50            | 120           | <i>a</i>     | 61.94   | 46.65     | 20.65     | 74.24   | 11,045      | 14.06       | 0.77 | 785.45  | 1745.42      |
|      |     | 50            | 120           | <i>b</i>     | 36.36   | 32.17     | 12.12     | 51.23   | 7660        | 7.98        | 0.56 | 959.97  |              |
| OP9  | OF4 | 50            | 120           | <i>a</i>     | 18.00   | 29.94     | 13.12     | 50.00   | 10,264      | 12.72       | 0.91 | 806.91  | 1696.45      |
|      |     | 50            | 120           | <i>b</i>     | 18.00   | 30.94     | 12.12     | 50.00   | 7400        | 8.32        | 0.64 | 889.53  |              |
| OP10 | OF5 | 50            | 120           | <i>a</i>     | 62.21   | 46.87     | 20.74     | 74.54   | 11,050      | 14.10       | 0.77 | 783.81  | 1742.31      |
|      |     | 50            | 120           | <i>b</i>     | 36.36   | 31.86     | 12.12     | 50.92   | 7643        | 7.97        | 0.56 | 958.50  |              |
| OP11 | OF6 | 50            | 120           | <i>a</i>     | 18.00   | 29.94     | 13.12     | 50.00   | 10,264      | 12.72       | 0.91 | 806.93  | 1696.45      |
|      |     | 50            | 120           | <i>b</i>     | 18.00   | 30.94     | 12.12     | 50.00   | 7400        | 8.32        | 0.64 | 889.52  |              |
| OP12 | OF2 | 40            | 120           | <i>a</i>     | 59.58   | 44.70     | 19.86     | 71.50   | 10,997      | 13.74       | 0.78 | 800.13  | 1809.87      |
|      |     | 40            | 120           | <i>b</i>     | 28.38   | 23.76     | 9.46      | 40.15   | 7276        | 7.21        | 0.60 | 1009.74 |              |

Table 3 (Continued)

| CS   | COF | $C_{\min}$<br>(s) | $C_{\max}$<br>(s) | Intersection | $D$<br>(m) | $g_1$<br>(s) | $g_2$<br>(s) | $C$<br>(s) | $Q$<br>(veh/h) | $d$<br>(s/veh) | $x$  | $Q/d$   | $\Sigma Q/d$ |
|------|-----|-------------------|-------------------|--------------|------------|--------------|--------------|------------|----------------|----------------|------|---------|--------------|
| OP13 | OF3 | 40                | 120               | <i>a</i>     | 61.94      | 46.64        | 20.65        | 74.23      | 11,045         | 14.06          | 0.77 | 785.48  | 1772.50      |
|      |     | 40                | 120               | <i>b</i>     | 33.15      | 29.29        | 11.05        | 47.28      | 7558           | 7.66           | 0.57 | 987.02  |              |
| OP14 | OF4 | 40                | 120               | <i>a</i>     | 18.00      | 22.99        | 10.08        | 40.00      | 9909           | 11.95          | 0.92 | 829.00  | 1795.93      |
|      |     | 40                | 120               | <i>b</i>     | 18.00      | 23.76        | 9.30         | 40.00      | 7157           | 7.40           | 0.63 | 966.93  |              |
| OP15 | OF5 | 40                | 120               | <i>a</i>     | 62.21      | 46.87        | 20.74        | 74.54      | 11,050         | 14.10          | 0.77 | 783.81  | 1776.12      |
|      |     | 40                | 120               | <i>b</i>     | 32.29      | 28.26        | 10.76        | 45.96      | 7512           | 7.57           | 0.57 | 992.31  |              |
| OP16 | OF6 | 40                | 120               | <i>a</i>     | 18.00      | 22.99        | 10.08        | 40.00      | 9909           | 11.95          | 0.92 | 829.02  | 1795.95      |
|      |     | 40                | 120               | <i>b</i>     | 18.00      | 23.76        | 9.30         | 40.00      | 7157           | 7.40           | 0.63 | 966.93  |              |
| OP17 | OF2 | 40                | 110               | <i>a</i>     | 59.58      | 44.70        | 19.86        | 71.50      | 10,997         | 13.74          | 0.78 | 800.13  | 1809.87      |
|      |     | 40                | 110               | <i>b</i>     | 28.38      | 23.76        | 9.46         | 40.15      | 7276           | 7.21           | 0.60 | 1009.74 |              |
| OP18 | OF3 | 40                | 110               | <i>a</i>     | 61.94      | 46.64        | 20.65        | 74.23      | 11,045         | 14.06          | 0.77 | 785.48  | 1772.51      |
|      |     | 40                | 110               | <i>b</i>     | 33.15      | 29.29        | 11.05        | 47.28      | 7558           | 7.66           | 0.57 | 987.03  |              |
| OP19 | OF4 | 40                | 110               | <i>a</i>     | 18.00      | 22.99        | 10.08        | 40.00      | 9909           | 11.95          | 0.92 | 829.00  | 1795.93      |
|      |     | 40                | 110               | <i>b</i>     | 18.00      | 23.76        | 9.30         | 40.00      | 7157           | 7.40           | 0.63 | 966.93  |              |
| OP20 | OF5 | 40                | 110               | <i>a</i>     | 62.21      | 46.87        | 20.74        | 74.54      | 11,050         | 14.10          | 0.77 | 783.80  | 1776.12      |
|      |     | 40                | 110               | <i>b</i>     | 32.29      | 28.26        | 10.76        | 45.96      | 7512           | 7.57           | 0.57 | 992.31  |              |
| OP21 | OF6 | 40                | 110               | <i>a</i>     | 18.00      | 22.99        | 10.08        | 40.00      | 9909           | 11.95          | 0.92 | 829.02  | 1795.95      |
|      |     | 40                | 110               | <i>b</i>     | 18.00      | 23.76        | 9.30         | 40.00      | 7157           | 7.40           | 0.63 | 966.93  |              |
| OP22 | OF2 | 40                | 100               | <i>a</i>     | 59.58      | 44.70        | 19.86        | 71.50      | 10,997         | 13.74          | 0.78 | 800.13  | 1809.89      |
|      |     | 40                | 100               | <i>b</i>     | 28.38      | 23.76        | 9.46         | 40.15      | 7276           | 7.21           | 0.60 | 1009.77 |              |
| OP23 | OF3 | 40                | 100               | <i>a</i>     | 61.94      | 46.64        | 20.65        | 74.23      | 11,045         | 14.06          | 0.77 | 785.48  | 1772.51      |
|      |     | 40                | 100               | <i>b</i>     | 33.15      | 29.29        | 11.05        | 47.28      | 7558           | 7.66           | 0.57 | 987.03  |              |
| OP24 | OF4 | 40                | 100               | <i>a</i>     | 18.00      | 22.99        | 10.08        | 40.00      | 9909           | 11.95          | 0.92 | 829.00  | 1795.93      |
|      |     | 40                | 100               | <i>b</i>     | 18.00      | 23.76        | 9.30         | 40.00      | 7157           | 7.40           | 0.63 | 966.93  |              |
| OP25 | OF5 | 40                | 100               | <i>a</i>     | 62.21      | 46.87        | 20.74        | 74.54      | 11,050         | 14.10          | 0.77 | 783.81  | 1776.12      |
|      |     | 40                | 100               | <i>b</i>     | 32.29      | 28.26        | 10.76        | 45.96      | 7512           | 7.57           | 0.57 | 992.31  |              |
| OP26 | OF6 | 40                | 100               | <i>a</i>     | 18.00      | 22.99        | 10.08        | 40.00      | 9909           | 11.95          | 0.92 | 829.02  | 1795.95      |
|      |     | 40                | 100               | <i>b</i>     | 18.00      | 23.76        | 9.30         | 40.00      | 7157           | 7.40           | 0.63 | 966.93  |              |

Note: CS and COF represent the code of scenario and the code of objective function, respectively.

#### 4. Model verification and validation

##### 4.1. Design of simulation scenarios

To further analyse the effects of different scenarios on traffic flow operations and validate the reliability of the optimization models, four scenarios CP, OP1, OP12 and OP16 are simulated by applying VISSIM software, here CP represents the existing scenario

from the above survey. The channelization and signal timing parameters of each scenario are listed in Table 4. Adopting the mode of multi-run in VISSIM, the simulation duration and the number of runs are set to 3600 and 10, respectively. Additionally, the *Node Evaluation* and *Link Evaluation* are adopted to test the impacts of these scenarios on traffic flow operations.

As indicated in Fig. 4, two nodes and four links will be evaluated. The nodes refer to the study intersections, and the links include the short-lane and normal-lane sections on the southbound approach at intersection *a* (name them Link 1 and Link 2) and the short-lane and normal-lane sections on the northbound approach at intersection *b* (name them Link 3 and Link 4). For the *Node Evaluation*, three evaluation parameters of cumulative vehicles, average delay and average queue length are selected. For the *Link Evaluation*, one evaluation parameter of average running speed is selected.

For an intersection, the more the cumulative count of vehicles traversing the intersection is, the lesser the average delay of vehicles traversing the intersection is, the shorter the average queue length on the approach is, or the quicker the average running speed of vehicles on the link is, the better the corresponding scenario is.

#### 4.2. Analysis of node and link evaluations

Table 5 indicates the results of node evaluation from VISSIM, and lists the cumulative vehicles and the average delay for each movement and all movements, and the average queue length on each approach and all approaches at intersections *a* and *b*. For intersection *a*, the cumulative vehicles under CP is the least, but the average delay and queue length are all the most; the cumulative vehicles under the other scenarios are slightly different; the average delays and queue lengths under OP12 and OP16 are all less than those under OP1; the cumulative vehicles, average delay and average queue length under OP12 are all more than those under OP16. For intersection *b*, the cumulative vehicles under all the scenarios are slightly different; the average delays and queue lengths under OP12 and OP16 are all less

Table 4. Channelization and signal timing parameters of the simulation scenarios

| Code of scenario | Intersection | Length of short lane (m) | Green time 1 (s) | Green time 2 (s) | Cycle length (s) |
|------------------|--------------|--------------------------|------------------|------------------|------------------|
| CP               | <i>a</i>     | 66                       | 79               | 31               | 120              |
|                  | <i>b</i>     | 33                       | 50               | 13               | 73               |
| OP1              | <i>a</i>     | 49                       | 49               | 15               | 74               |
|                  | <i>b</i>     | 28                       | 51               | 8                | 69               |
| OP12             | <i>a</i>     | 60                       | 43               | 18               | 71               |
|                  | <i>b</i>     | 28                       | 22               | 8                | 40               |
| OP16             | <i>a</i>     | 18                       | 21               | 9                | 40               |
|                  | <i>b</i>     | 18                       | 22               | 8                | 40               |

Note: Green time means the duration of the green indication for a phase, and is equal to the effective green time plus the start-up lost time and then minus the amber time for the phase.

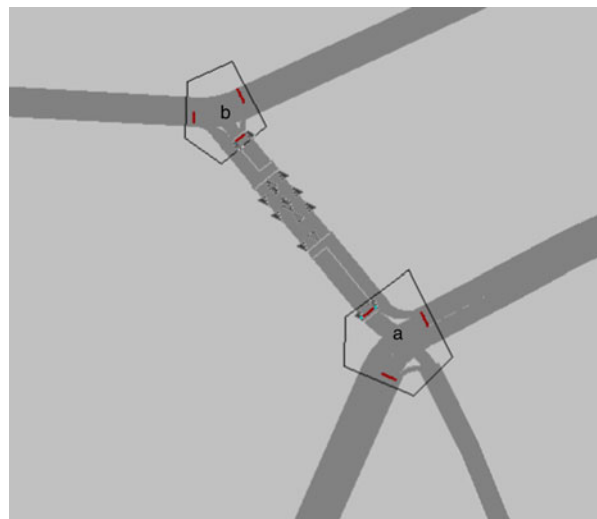


Fig. 4. Settings of node and link evaluations in VISSIM

than those under CP and OP1; the cumulative vehicles, average delay and average queue length under OP12 are all slightly less than those under OP16.

Table 6 shows the results of link evaluation from VISSIM, and lists the average running speed on each selected link at intersections *a* and *b*. It can be seen that the average running speeds on Links 1, 2 and 3 under OP12 are all the highest, the average running speed on Link 4 under OP12 is slightly less than that under OP16; OP12 and OP16 all improve the average running speeds of vehicles on all links except Link 1 under OP16 when comparing with CP.

#### 4.3. Comparison between optimization and simulation results

Table 7 compares the optimization results with the simulation results for OP1, OP12 and OP16. The capacity of intersections *a* and *b* under different scenarios is clearly different. The capacity under OP1 is the greatest, the capacity under OP16 is the least, and the capacity under OP12 takes the second place. However, the cumulative counts of vehicles passing through intersections *a* and *b* under different scenarios are all very close. According to the average delay or the capacity to delay ratio, the ordered sequence of these three scenarios obtained from the optimization results is identical to that from the simulation results for intersections *a* and *b*. It is indicated that the greater the capacity to delay ratio of a scenario from the proposed optimization model is, the better is the control effect of this scenario in practice.

### 5. Model application

#### 5.1. Discussions and suggestions

For intersections *a* and *b* as a whole, Table 8 lists the total cumulative vehicles, average delay, average queue length and total cumulative vehicles to average

Table 5. Results of node evaluation from VISSIM

| Intersection <i>a</i> |          |              |              |               |                |               |        |
|-----------------------|----------|--------------|--------------|---------------|----------------|---------------|--------|
|                       | Scenario | East to west | West to east | North to east | North to south | East to north | All    |
| Cumulative vehicles   | CP       | 2515.3       | 3431.6       | 871.6         | 859.4          | 604.6         | 8282.5 |
|                       | OP1      | 2537.7       | 3461.7       | 861.3         | 849.4          | 604.6         | 8314.7 |
|                       | OP12     | 2537.7       | 3461.7       | 861.9         | 849.3          | 604.6         | 8315.2 |
|                       | OP16     | 2530.9       | 3451.5       | 867.5         | 856.5          | 604.6         | 8311.0 |
|                       | Scenario | East to west | West to east | North to east | North to south | East to north | All    |
| Average delay         | CP       | 9.22         | 9.97         | 37.69         | 38.67          | 0.20          | 14.92  |
|                       | OP1      | 5.77         | 6.44         | 30.99         | 29.44          | 0.20          | 10.69  |
|                       | OP12     | 7.38         | 8.18         | 23.29         | 23.76          | 0.19          | 10.50  |
|                       | OP16     | 6.27         | 7.22         | 23.18         | 17.58          | 0.19          | 9.17   |
|                       | Scenario | Eastern      | Western      | Northern      | All            |               |        |
| Average queue length  | CP       | 10.99        | 17.52        | 30.61         | 19.72          |               |        |
|                       | OP1      | 5.69         | 8.61         | 24.52         | 12.95          |               |        |
|                       | OP12     | 7.57         | 11.67        | 19.24         | 12.83          |               |        |
|                       | OP16     | 5.47         | 8.20         | 8.65          | 7.45           |               |        |
|                       | Scenario | Eastern      | Western      | Northern      | All            |               |        |
| Intersection <i>b</i> |          |              |              |               |                |               |        |
|                       | Scenario | East to west | West to east | South to west | West to south  | All           |        |
| Cumulative vehicles   | CP       | 1215.7       | 1649.1       | 599.6         | 1740.1         | 5204.5        |        |
|                       | OP1      | 1214.5       | 1647.9       | 600.8         | 1740.8         | 5204.0        |        |
|                       | OP12     | 1212.3       | 1646.1       | 602.1         | 1740.7         | 5201.2        |        |
|                       | OP16     | 1212.3       | 1646.1       | 602.1         | 1740.8         | 5201.3        |        |
|                       | Scenario | East to west | West to east | South to west | West to south  | All           |        |
| Average delay         | CP       | 4.28         | 4.73         | 27.24         | 0.99           | 5.97          |        |
|                       | OP1      | 3.05         | 3.11         | 34.60         | 0.74           | 5.94          |        |
|                       | OP12     | 5.09         | 5.45         | 15.45         | 0.64           | 4.92          |        |
|                       | OP16     | 5.09         | 5.45         | 15.44         | 0.66           | 4.94          |        |
|                       | Scenario | Eastern      | Western      | Southern      | All            |               |        |
| Average queue length  | CP       | 2.82         | 3.79         | 12.17         | 6.92           |               |        |
|                       | OP1      | 1.81         | 2.14         | 14.71         | 7.11           |               |        |
|                       | OP12     | 3.08         | 3.81         | 6.94          | 4.90           |               |        |
|                       | OP16     | 3.08         | 3.81         | 6.94          | 4.92           |               |        |
|                       | Scenario | Eastern      | Western      | Southern      | All            |               |        |

delay ratio under each simulation scenario. It can be seen that all the optimization scenarios increase the total cumulative vehicles, and the total cumulative vehicles to average delay ratio, decrease the average delay and the average queue length when comparing with CP; the total cumulative vehicles under OP1,

OP12 and OP16 have only slight difference, the average delays and the average queue lengths under OP12 and OP16 are all less than those under OP1, the total cumulative vehicles to average delay ratios under OP12 and OP16 are all more than those under OP1.

Table 6. Results of link evaluation from VISSIM

| Scenario | Southbound approach at intersection <i>a</i> |                        | Northbound approach at intersection <i>b</i> |                        |
|----------|--|------------------------|--|------------------------|
|          | Speed on Link 1 (km/h)                       | Speed on Link 2 (km/h) | Speed on Link 3 (km/h)                       | Speed on Link 4 (km/h) |
| CP       | 5.78   | 39.23                  | 4.30   | 43.22                  |
| OP1      | 5.62   | 41.07                  | 3.09   | 41.99                  |
| OP12     | 8.18   | 42.84                  | 6.61   | 44.64                  |
| OP16     | 5.41   | 39.53                  | 4.62   | 44.64                  |

Thus, the following recommended objective functions and parameter values are put forward, as listed in Table 9. For an actual situation, the parameter values in Table 9 can somewhat vary.

### 5.2. Procedure of using the models

The above-mentioned model optimization focusses on a one-hour analysis period. As we all know, traffic flow fluctuates within the whole day, and multiple analysis periods are usually created for signalized intersections, and different signal timing plans are often adopted for different analysis periods. However, the channelization scheme for an intersection often remains stable during a longer period, such as several months or years. Thus, it is necessary to illustrate the application of the recommended models in practice. The detailed steps are as follows:

- **Step 1:** According to the variation curves of traffic volumes at intersections *a* and *b* on a selected typical weekday during a study period, split several suitable timing phases and name them *Phase 1*, *Phase 2*, *Phase 3*...
- **Step 2:** For *Phase 1*, *Phase 2*, *Phase 3*..., using the corresponding peak 5-min flow rates and adopting one or more of the

objective functions in *Category 1* to optimize equations (12) or (13), the obtained optimal scenarios are denoted as *Scenario A1*, *Scenario A2*, *Scenario A3*...

- **Step 3:** For *Phase 1*, *Phase 2*, *Phase 3*..., using the corresponding peak 5-min flow rates and adopting one or more of the objective functions in *Category 2* to optimize equation (13), the obtained optimal scenarios are denoted as *Scenario B1*, *Scenario B2*, *Scenario B3*...
- **Step 4:** For the study period, if the road space is sufficient for intersections *a* and *b*, select the maxima of the SL lengths from all the optimal scenarios in **Step 2** to channelize the left-turn bays.
- **Step 5:** For the study period, if the road space is very limited for intersections *a* and *b*, select the maxima of the SL lengths from all the optimal scenarios in **Step 3** to channelize the left-turn bays.
- **Step 6:** If the left-turn bays are channelized based on **Step 4**, select the corresponding optimal timing plan in **Step 2** for each phase to practice.
- **Step 7:** If the left-turn bays are channelized based on **Step 5**, select the corresponding optimal timing plan in **Step 3** for each phase to practice.

### Conclusions

SLs, which are often channelized at signalized intersections have an important effect on approach capacity. The correlated SLs, which sometimes exist on the common section between two adjacent intersections, can have an impact on each other. Focussing on two adjacent intersections, which are not coordinated by traffic signals and according to the impact of a short lane on approach capacity, three kinds of multi-objective optimization models are

Table 7. Comparison between optimization and simulation results

| Scenario | Intersection | Capacity (veh/h) <sup>a</sup> |                    | Average delay (s/veh) |                    | Capacity to delay ratio <sup>b</sup> |                    |
|----------|--------------|-------------------------------|--------------------|-----------------------|--------------------|--------------------------------------|--------------------|
|          |              | Optimization results          | Simulation results | Optimization results  | Simulation results | Optimization results                 | Simulation results |
| OP1      | <i>a</i>     | 11,377.0                      | 8314.7             | 17.31                 | 10.69              | 657.22                               | 777.80             |
|          | <i>b</i>     | 8592.3                        | 5204.0             | 14.63                 | 5.94               | 587.50                               | 876.09             |
| OP12     | <i>a</i>     | 10,997.0                      | 8315.2             | 13.74                 | 10.50              | 800.13                               | 791.92             |
|          | <i>b</i>     | 7276.3                        | 5201.2             | 7.21                  | 4.92               | 1009.74                              | 1057.15            |
| OP16     | <i>a</i>     | 9908.8                        | 8311.0             | 11.95                 | 9.17               | 829.02                               | 906.32             |
|          | <i>b</i>     | 7156.7                        | 5201.3             | 7.40                  | 4.94               | 966.93                               | 1052.89            |

<sup>a</sup>For the simulation scenarios, the capacity means the cumulative counts of vehicles passing through the intersection per hour.

<sup>b</sup>For the simulation scenarios, the capacity to delay ratio means the ratio of the cumulative counts of vehicles passing through the intersection per hour to the average delay of these vehicles.

Table 8. Results of node evaluation for intersections *a* and *b* as a whole

| Scenario | Total cumulative vehicles (veh/h) | Average delay (s/veh) | Average queue length (m) | Total cumulative vehicles to average delay ratio |
|----------|-----------------------------------|-----------------------|--------------------------|--|
| CP       | 13,487                            | 11.47                 | 13.91                    | 1175.85  |
| OP1      | 13,519                            | 8.85                  | 10.27                    | 1527.54  |
| OP12     | 13516                             | 8.37                  | 9.23                     | 1614.86  |
| OP16     | 13,512                            | 7.54                  | 6.29                     | 1792.08  |

built in this paper. As the solutions to these models depend on their concrete objective functions, the feasible objective functions are given, based on operations research, and then the corresponding solution method is also presented. By using the 2010 field data from the city of Dalian, China, the sensitivity of these models to the parameters (critical cycle lengths) is emphatically analyzed. Also, to verify the improvement of traffic flow operations resulted from the optimization scenarios, the current scenario and three typical optimization ones are simulated by using *VISSIM* software. Considering the optimization and simulation outcomes synthetically, the better optimization models, which are classified into two categories and the corresponding parameter values are suggested to apply to practical engineering. Finally, the application procedure of the recommended models is introduced.

To sum up, this paper gains the following progress. First of all, three kinds of optimization models are proposed to optimally allocate time and space resources for two adjacent intersections as a whole. Next, based on the results of the sensitivity analysis of these models, the better models and the suitable parameter values or ranges are found. At last, the detailed steps of using the recommended models are given.

Table 9. Recommended objective functions and parameter values

| Category | Objective function   | Minimum cycle length (s) | Maximum cycle length (s) |
|----------|--|--------------------------|--------------------------|
| 1        | minimize $(d_a + d_b)$<br>maximize $(Q_a + Q_b)/(d_a + d_b)$<br>maximize $(Q_a/d_a + Q_b/d_b)$ | 40                       | 120                      |
| 2        | minimize $(d_a + d_b)/(Q_a + vQ_b)$<br>minimize $(d_a/Q_a + d_b/Q_b)$                          |                          |                          |

But then, when the distance between two adjacent intersections is shorter than  $750 \div 1000$  metres, and one or more of traffic movements at one intersection are relative to one or more of ones at the other intersection, the intersections could not be regarded as isolated intersections. Then the signal coordination has to be considered. This case will be discussed in another paper by improving the models in this one.

**Acknowledgment**

The research reported in this paper was supported by the National Natural Science Foundation of China (Grant no. 50808035).

**References**

*Highway Capacity Manual*. 2000. Transportation Research Board, National Research Council. 1134 p.

Jiang, J.; Yang, P. 2008. Capacity at a signalized intersection approach with short lanes related to the cycle length, in *Plan, Build, and Manage Transportation Infrastructure in China: Proceedings of the Seventh International Conference of Chinese Transportation Professionals (ICCTP)*, May 21–22, 2007, Shanghai, China, 575–582. [http://dx.doi.org/10.1061/40952\(317\)56](http://dx.doi.org/10.1061/40952(317)56)

Kikuchi, S.; Chakroborty, P.; Vukadinovic, K. 1993. Lengths of left-turn lanes at signalized intersections, *Transportation Research Record* 1385: 162–171.

Kikuchi, S.; Kii, M.; Chakroborty, P. 2004. Lengths of double or dual left-turn lanes, *Transportation Research Record* 1881: 72–78. <http://dx.doi.org/10.3141/1881-09>

Kikuchi, S.; Kronprasert, N. 2010. Determining lengths of left-turn lanes at signalized intersections under different left-turn signal schemes, *Transportation Research Record* 2195: 70–81. <http://dx.doi.org/10.3141/2195-08>

Kikuchi, S.; Kronprasert, N.; Kii, M. 2007. Lengths of turn lanes on intersection approaches: three-branch fork lanes – left-turn, through, and right-turn lanes, *Transportation Research Record* 2023: 92–101. <http://dx.doi.org/10.3141/2023-10>

Klibavicius, A.; Paliulis, G.-M.; Muench, H. 2008. Simulation of short lane capacity for reconstruction of intersections, in *The 7th International Conference “Environmental Engineering”: Selected Papers*, Vol. 3, May 22–23, 2008 Vilnius, Lithuania, 981–986.

Lee, J.-J.; Roupail, N. M.; Hummer, J. E. 2005. Models for lane utilization prediction for lane drop intersections, *Transportation Research Record* 1912: 47–56. <http://dx.doi.org/10.3141/1912-06>

Qi, Y.; Yu, L.; Azimi, M.; Guo, L. 2007. Determination of storage lengths of left-turn lanes at signalized intersections, *Transportation Research Record* 2023: 102–111. <http://dx.doi.org/10.3141/2023-11>

Road and Transportation Research Association. 2003. *Guidelines for Traffic Signals (RiLSA)*. 182 p.

Tian, Z.; Wu, N. 2006. Probabilistic model for signalized intersection capacity with a short right-turn lane, *Journal of Transportation Engineering* 132(3): 205–212. [http://dx.doi.org/10.1061/\(ASCE\)0733-947X\(2006\)132:3\(205\)](http://dx.doi.org/10.1061/(ASCE)0733-947X(2006)132:3(205))

- Wu, N. 1999. Capacity of shared-short lanes at unsignalized intersections, *Transportation Research Part A: Policy and Practice* 33(3–4): 255–274.  
[http://dx.doi.org/10.1016/S0965-8564\(98\)00041-X](http://dx.doi.org/10.1016/S0965-8564(98)00041-X)
- Wu, N. 2007. Total approach capacity at signalized intersections with shared and short lanes: generalized model based on a simulation study, *Transportation Research Record* 2027: 19–26.  
<http://dx.doi.org/10.3141/2027-03>
- Wu, B.; Li, Y. 2009. *Traffic Management and Control*. 4th edition. Beijing: China Communications Press.
- Yao, R. H.; Wang, J. L.; Wang, T. C.; Zhu, C. G. 2011. Synergistic optimization model of length of left-turn short lane and signal timing parameters, *Transport Standardization* (9): 167–171.